Postcollision interaction and two-center effects in ionizing collisions

L. Sarkadi,* L. Gulyás, and L. Lugosi
Institute of Nuclear Research of the Hungarian Academy of Sciences (ATOMKI), P.O. Box 51, H-4001 Debrecen, Hungary
(Received 4 January 2002; published 3 May 2002)

Momentum distributions of the recoil target ion and the ejected electron have been calculated for 75-keV $H_2^+ + He$ collisions by applying the classical trajectory Monte Carlo (CTMC) and the continuum-distorted-wave-eikonal-initial-state (CDW-EIS) theory. A qualitative agreement was found between the calculated centroid values of the momentum distributions and the corresponding experimental data published recently by An *et al.* [Phys. Rev. A **63**, 030703 (2001)]. The presence of postcollision interaction effects in the momentum distributions was analyzed repeating the CTMC calculations with a short-range model potential between the electron and the projectile ion as a function of the interaction length. The role of two-center effects was investigated by comparing the CDW-EIS results with those obtained in the first-Born approximation.

DOI: 10.1103/PhysRevA.65.052715 PACS number(s): 34.50.Fa, 34.50.Bw, 34.10.+x

I. INTRODUCTION

The process of *electron capture to the continuum* (ECC) has received much attention in the physics of energetic ion-atom collisions since its discovery [1–3]. ECC can be viewed as a continuation of the electron capture into high-lying bound states (Rydberg states) of the projectile over the ionization threshold: The process leads to population of the low-energy continuum states around the projectile. The electrons ''captured'' to the continuum of the projectile form a pronounced cusp-shaped peak in the energy spectrum of the forward ejected electrons at an energy that corresponds to $v_e = v_p$, where v_e and v_p are the velocities of the electron and projectile, respectively. The phenomenon of cusp-electron emission is particularly interesting, mainly because it is a *postcollision interaction* (PCI) effect: The cusp is formed as a result of the *long-range* Coulomb interaction between the ionized electron and the outgoing charged projectile. Furthermore, the properties (intensity, asymmetry, etc.) of the cusp peak are also influenced by the ionized target atom, i.e., the cusp can be understood only if one considers the full three-body (electron, target core, projectile) dynamics of the collision. On this ground the cusp is regarded as a *two-center* electron emission [4].

The cusp peak appearing in the electron spectrum is a direct manifestation of ECC. The measurement of the energy (and angular) distribution of the electrons is relatively simple, i.e., ECC can be effectively studied experimentally by determining doubly differential cross sections (DDCS) for the electron emission around the matching velocity $\vec{v}_e = \vec{v}_p$. This explains why most of the experimental investigations of ECC were carried out by measuring the electron cusp.

At the same time, ECC is reflected also in the momentum distributions of the other two collision fragments (the scattered projectile and the recoil target ion). However, due to the large projectile-to-electron and target-to-electron mass ratios the effect for the heavy fragments is much smaller than for the electron. The presence of ECC (or, in general, the PCI effect) in the momentum spectra of the projectile and the recoil target ion was observed only recently [5–9]. Such observations became possible applying different experimental techniques, particularly the recoil ion momentum spectroscopy (for a review see Ullrich *et al.* [10]).

Here we report on a theoretical investigation of ECC in which we attempted to interpret the recent experimental results obtained by An *et al.* [9]. These authors performed a kinematically complete experiment on single ionization for 75-keV $H_2^+ + He$ collisions by combining the techniques of the projectile energy-loss spectrometry and the recoil ion momentum spectroscopy. The momentum vectors of the heavy collision products were determined by detecting the fully momentum analyzed projectiles and the recoil ions in coincidence. The electron momentum was deduced from momentum conservation. The authors analyzed the *centroids* of the longitudinal and transverse momentum distributions for both the recoil ions and ejected electrons as a function of the energy loss of the projectile. They considered the case of 0° projectile scattering angle. It was found that the momentum distributions of the collision products, especially for the electron, show clear signatures of PCI.

An *et al.* explained their experimental findings only qualitatively, without comparing the data with theoretical calculations. In the present work we gave a quantitative analysis of the problem by performing calculations within the framework of the *classical trajectory Monte Carlo* (CTMC) model and the *continuum distorted wave* (CDW) theory. We show that although the gross tendencies of the momentum distributions as a function of the energy loss of the projectile can simply be explained by kinematical effects, the rapid changes of the momentum centroids observed in the experiment at the energy-loss value corresponding to the matching velocity $v_e = v_p$ are indeed signatures of PCI. In our analysis we could determine the effects of PCI in the momentum distributions by repeating the CTMC calculations with a *short-range* interaction potential between the electron and the projectile ion. These calculations were made at several interaction length values. In addition to PCI, we investigated also the contributions due to two-center character of the electron emission. In order to identify these latter effects, we compared the results of the CDW calculations with those

*Email address: sarkadil@atomki.hu

 ©2002 The American Physical Society

obtained in the first-Born approximation (i.e., a theory that accounts only for the one-center electron emission).

II. THEORY

In both theoretical calculations (CTMC and CDW) we regarded a simplified collision system. The H_2^+ projectile was replaced by a pointlike charged particle of identical mass. The effective charge of the particle, Z_p, was determined from the ionization potential of the H_2 molecule, assuming the $I=1/2Z_p^2$ hydrogenic relationship (in atomic units). This gives $Z_p=1.064$.

The calculations were made in the *independent-particle model*, i.e., the electron correlation effects were neglected. This means that the He atom was replaced by a one-electron atom in which the electron moves in an effective field of the He^+ ion core. In the CTMC simulations the ion core was represented by a model potential developed by Green *et al.* [11] based on Hartree-Fock calculations. The potential has the following form for a neutral atom:

$$V(r)=-[(Z-1)\Omega(r)+1]/r, \tag{1}$$

where Z is the nuclear charge and

$$\Omega(r)=\{(\eta/\xi)[\exp(\xi r)-1]+1\}^{-1}.$$

The values of η and ξ were taken from Garvey *et al.* [12]. For He $\eta=1.77$ and $\xi=2.625$.

Details of our procedure applying the CTMC method for the description of various atomic collision processes can be found in previous works [13–19], therefore, here we summarize only the main points of the theory. The method is based on the numerical solution of Newton's classical equations of motion for a large number of trajectories under randomly chosen initial conditions [20,21]. CTMC has the advantage that it treats the three- (many-) body dynamics exactly. This is particularly important for the description of processes influenced by PCI effects.

We applied the three-body version of the CTMC theory: The equations of motion were solved for the projectile, the active electron, and the target core. The calculations were made in two steps. In the first step the equations of motion were integrated until the main reaction channels (excitation, ionization, electron capture to bound states of the projectile) were well separated. This condition was fulfilled at an internuclear distance of 25 a.u. In the second step only collision events leading to ionization were regarded. Since we were interested in PCI effects (including the formation of the electron cusp), we integrated the equations of motion in the final ionization channel over a large internuclear separation, up to 10^5 a.u.

The CDW calculations were made in the CDW-EIS (continuum-distorted-wave-eikonal-initial-state) approximation. This model is known to be a very efficient theory for the description of the continuous electron ejection in ion-atom collisions (see, e.g., Fainstein *et al.* [4]). The ejected electron is described by a two-center wave function, therefore, the model gives account of the two-center effects in the electron emission (including ECC). The applied CDW-EIS model [22] assumes straight-line trajectory for the projectile path and uses Hartree-Fock-Slater wave functions for the initial and final electronic states.

III. RESULTS AND DISCUSSION

The centroids of the momentum distributions obtained from the CTMC and CDW-EIS calculations as a function of the projectile energy loss ΔE_p are compared with the measured data of An *et al.* [9] in Fig. 1. In part (a) of the figure results for the longitudinal momentum of the recoil target ion are plotted, in parts (b) and (c) those for the longitudinal and transverse momentum of the ejected electron are shown, respectively. We note that the measured centroid values of the longitudinal electron momentum distributions were probably obtained by an erroneous data evaluation procedure: They are inconsistent with the data sets of the other two momentum distributions regarding the energy and momentum conservation. However, multiplying these data by a factor of three, we obtained results that are consistent with the other experimental data, as well as very close to the calculated centroid values. In Fig. 1(b) we plotted both the original and the corrected experimental data.

The CTMC results seen in the figure were obtained running our CTMC computer code for 2×10^7 collision events. We had to regard such large number of collision events for the following reason. The experiment was performed with high energy and angular resolution for the scattered projectile: 1.2-eV full width at half maximum (FWHM) for the energy loss and 0.15-mrad FWHM for the angular scattering. In our ''computer play'' the windows for the energy loss and scattering angle of the projectile had to be chosen according to the experimental resolutions. These small windows strongly restricted the number of ionization events, particularly in the range of $\Delta E_p>45$ eV ($\Delta E_p=45$ eV corresponds to the matching electron velocity $v_e=v_p$). To achieve a reasonable statistical accuracy, in the evaluation of the CTMC data we used windows that were twice as large as the experimental resolutions. The use of larger windows did not change the centroids of the momenta appreciably.

The CDW-EIS results in the figure belong exactly to 0° projectile scattering angle, i.e., the triply differential cross section was not integrated over the angular range of the scattered projectile defined by the experimental resolution. This ''peaking'' approximation can be justified again by the very small value of the angular window (0.15 mrad) used in the experiment.

In Fig. 1 we plotted also the kinematical limits of the momentum distributions corresponding to 0° projectile scattering angle. These limits can be obtained from the energy and momentum conservation:

$$\vec{p}_p'+\vec{p}_a'=\vec{p}_p+\vec{p}_e+\vec{p}_t, \tag{2}$$

$$E_p'+E_a'=E_p+E_a^*+E_e+E_t. \tag{3}$$

Here $\vec{p}_p'$ and $\vec{p}_p$ are the momentum of the projectile before and after the collision, respectively, and E_p' and E_p are the corresponding kinetic energy of the projectile. $\vec{p}_e$ and $\vec{p}_t$ are

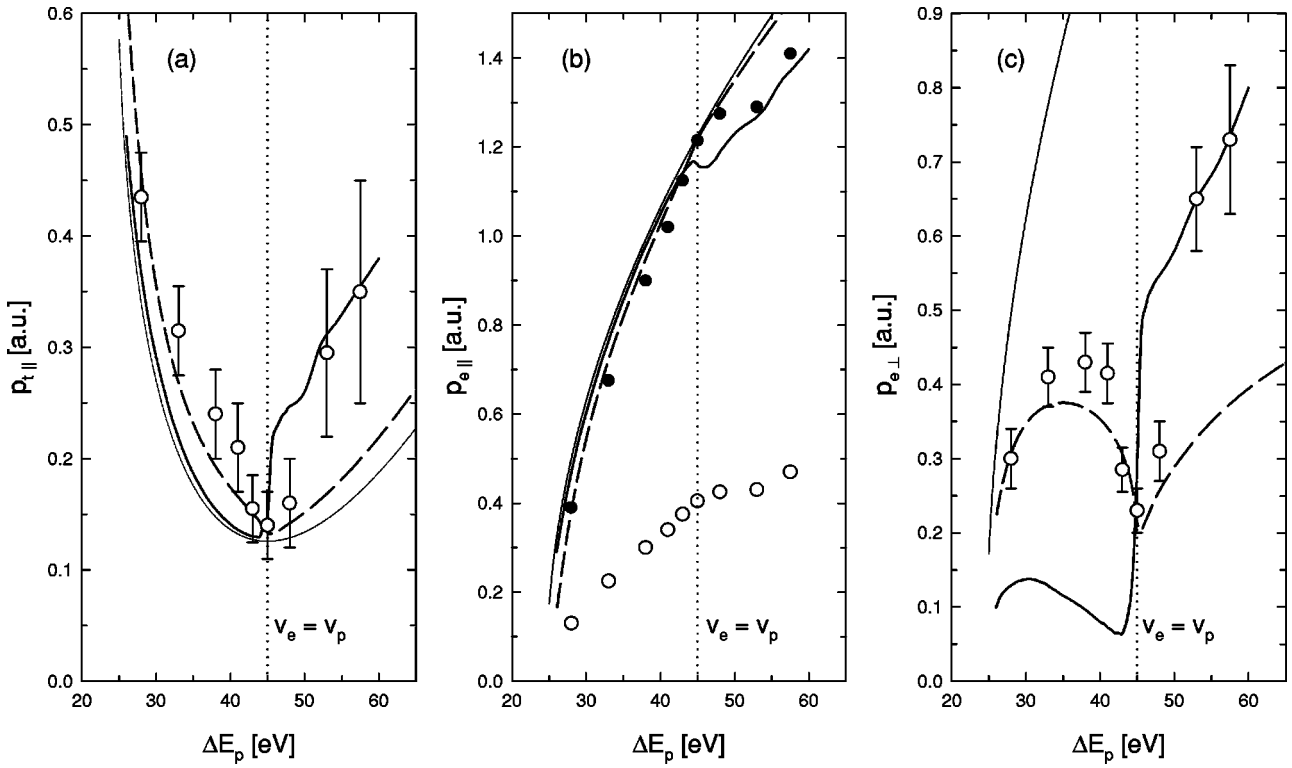

FIG. 1. Centroids of the momentum distributions of the recoil target ion and the ejected electron as a function of the projectile energy loss for 75-keV $H_2^+ + He$ collisions. (a) and (b) Longitudinal momentum of the target ion and the electron, respectively. (c) Transverse momentum of the electron. Experimental data: open circles, An *et al.* [9]; full circles, the $p_{e\parallel}$ data of An *et al.* multiplied by a factor of 3. Theories: solid line, CTMC; dashed line, CDW-EIS; thin solid line, kinematical limits.

the momenta of the ejected electron and the recoil target ion, respectively, E_e and E_t are the corresponding kinetic energies. Initially the target atom is in rest, therefore, its momentum $\vec{p}'_a = 0$. E'_a and E^*_a are the inner energy of the target atom before and after the collision, respectively. The difference $E^*_a - E'_a$ is the ionization potential I. The energy loss of the projectile is defined as

$$\Delta E_p \equiv E'_p - E_p = I + E_e + E_t . \tag{4}$$

For 0° projectile scattering angle Eq. (2) yields the following two equations for the momentum components parallel and perpendicular to the incoming ion-beam direction:

$$p'_{p\parallel} = p_{p\parallel} + p_{e\parallel} + p_{t\parallel} , \tag{5a}$$

$$0 = p_{e\perp} + p_{t\perp} . \tag{5b}$$

Here we used that $\vec{p}'_a = 0$, $p'_{p\perp} = 0$, and $p_{p\perp} = 0$.

Since for fast ion-atom collisions $\Delta E_p \ll E'_p$, we can express ΔE_p expanding $E'_p = p'^2_p/(2m_p)$ into Taylor series around $E_p = p_p^2/(2m_p)$. Here m_p is the mass of the projectile. We obtain in the first-order approximation

$$\Delta E_p = \frac{p'^2_p}{2m_p} - \frac{p_p^2}{2m_p} \approx \frac{p_p(p'_p - p_p)}{m_p}$$
$$\approx v(p'_p - p_p) = v_p(p'_{p\parallel} - p_{p\parallel}), \tag{6}$$

where v_p is the *initial* velocity of the projectile. By combining Eqs. (5a) and (6), we have

$$\frac{\Delta E_p}{v_p} = p_{e\parallel} + p_{t\parallel} . \tag{7}$$

Equation (4) gives another relationship between ΔE_p and the momentum components of the ejected electron and the recoil target ion,

$$\Delta E_p = I + \frac{p_{e\parallel}^2 + p_{e\perp}^2}{2m_e} + \frac{p_{t\parallel}^2 + p_{t\perp}^2}{2m_t}, \tag{8}$$

where m_e and m_t denote the mass of the electron and the target ion, respectively. Due to the large mass of the target ion, the third term here can be neglected. Denoting the electron emission angle by ϑ_e, we have

$$\Delta E_p \approx I + \frac{p_{e\parallel}^2 + p_{e\perp}^2}{2m_e} = I + \frac{p_{e\parallel}^2}{2m_e \cos^2 \vartheta_e} = I + \frac{p_{e\perp}^2}{2m_e \sin^2 \vartheta_e} . \tag{9}$$

By using Eqs. (5b), (7), and (9) the longitudinal momentum of the recoil target ion, as well as the longitudinal and transverse momenta of the ejected electron can be expressed as a function of the projectile energy loss and the electron emission angle:

$$p_{t\|}=\frac{\Delta E_p}{v_p}-\cos\vartheta_e\sqrt{2m_e(\Delta E_p-I)}, \tag{10a}$$

$$p_{e\|}=\cos\vartheta_e\sqrt{2m_e(\Delta E_p-I)}, \tag{10b}$$

$$p_{e\perp}=\sin\vartheta_e\sqrt{2m_e(\Delta E_p-I)}. \tag{10c}$$

The kinematical limits shown in Fig. 1 were obtained evaluating the above expressions at $\vartheta_e=0°$ for $p_{t\|}$ and $p_{e\|}$ and at $\vartheta_e=90°$ for $p_{e\perp}$.

In Figs. 1(a) and 1(b) both the experimental and theoretical momentum centroid values follow the curves belonging to the kinematical limits. This means that the gross tendencies of the $p_{t\|}$ and $p_{e\|}$ momentum centroids observed as a function of the energy loss of the projectile can simply be explained by the kinematics of the collision and by the fact that the angular distribution of the electron emission has a maximum close to $\vartheta_e=0°$ (especially for electron energies smaller than the cusp energy). At the same time, the abrupt deviations from the kinematical limits seen at higher values of the energy loss ($\Delta E_p>45$ eV) may partly be attributed to PCI. For $\Delta E_p<45$ eV CDW-EIS gives a better description of the experimental data than CTMC for both the $p_{t\|}$ and $p_{e\|}$ momentum centroids. In turn, at higher energy-loss values CTMC reproduces the measured data better than CDW-EIS.

On contrary to the $p_{t\|}$ and $p_{e\|}$ momentum distributions, the centroid values of $p_{e\perp}$ do not follow the kinematical limit [see Fig. 1(c)]. The reason is that in this case the limit belongs to electron emission angle $\vartheta_e=90°$, and the majority of the collision events are characterized with an emission angle $\vartheta_e<90°$. Both theory accounts the sudden drop occurring in the transverse electron momentum at $\Delta E_p=45$ eV. An *et al.* [9] explained this drop as a focusing effect: The attractive PCI focuses the ejected electrons toward the projectile. The focusing effect has a maximum for the cusp-electron emission at $v_e=v_p$, leading to a minimum of the transverse electron momentum. Here, again, for $\Delta E_p<45$ eV CDW-EIS gives almost a perfect description of the measured data, while CTMC strongly underestimates them. At higher energy-loss values the performance of the two theories is opposite.

We notice that the CDW-EIS curves in Figs. 1(a) and 1(c) are almost symmetric with respect to the $v_e=v_p$ line. This is in disagreement with the strong asymmetry of the experimental data around $v_e=v_p$: The measured $p_{t\|}$ and $p_{e\perp}$ momentum centroids rapidly increase above $v_e=v_p$. On the basis of this observation one may think that the disagreement between the CDW-EIS theory and the experiment is somehow related to the fact that this theory is unable to predict the asymmetry of the ECC cusp in the electron spectrum (see, e.g., Závodszky *et al.* [23]). Interestingly, the symmetry or asymmetry of the electron cusp does not determine unambiguously the behavior of the momentum centroids around $v_e=v_p$. We came to this conclusion by applying the CDW theory (i.e., *without* the ''EIS'' approximation) for calculation of the momentum centroids. The electron cusp predicted by this theory for bare ion projectiles is asymmetric, in accordance with the observations. Surprisingly, in spite of the difference in the shapes of the cusp, the momentum centroid values obtained by CDW and CDW-EIS were almost identical.

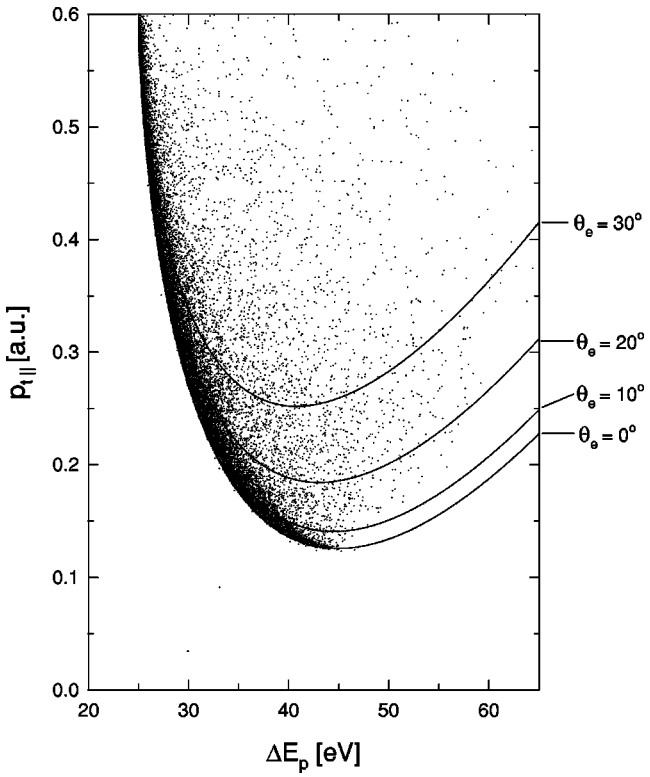

FIG. 2. Distribution of the ionizing collision events in the ΔE_p–$p_{t\|}$ plane obtained from the CTMC calculations. Solid lines: Eq. (10a) for electron emission angles of $\vartheta_e=0°$, 10°, 20°, and 30°.

We also notice that in a realistic calculation one should consider the electron on the H_2^+ projectile. This electron may actively participate in the collision, for example, it may polarize the electric field around the projectile. Such an effect may influence the momentum distributions of the collision fragments significantly.

The important role played by the kinematics of the collision in the behavior of the momentum centroids is well demonstrated by the map plotted in Fig. 2. Here each point in the ΔE_p–$p_{t\|}$ plane represents an individual ionizing collision event resulted by the CTMC calculations. The lines show the relationship (10a) between $p_{t\|}$ and ΔE_p for electron emission angles of $\vartheta_e=0°$, 10°, 20°, and 30°. For $\Delta E_p<45$ eV the majority of the points lie very close to kinematical limit defined by the $\vartheta_e=0°$ curve. We note that the collision events in the figure belong to $\vartheta_p=0°$ projectile scattering angle (within the angular window of 0.3 mrad). A similar behavior can be observed for the distribution of the longitudinal electron momentum component (not shown here).

In order to separate the contribution of PCI to the momentum distributions we made the following CTMC analysis. We were interested, first of all, in the formation of the electron cusp. The process was first investigated in the framework of the CTMC approach by Reinhold and Olson [24]. These authors studied the convergence of the cross section

for the cusp-electron emission as a function of the internuclear separation. For 100-keV protons on He collisions they found that full convergence was achieved for internuclear separations as large as 10^5 a.u. This result clearly proved that the electron cusp is a PCI phenomenon.

Our analysis was similar to that of Reinhold and Olson. We introduced the following model potential for the projectile-electron interaction:

$$V_{pe}(r) = -\frac{Z_p}{r}\exp\left[-\frac{r/r_c}{1+(r_c/r)^2}\right]. \tag{11}$$

In the limit $r_c \to \infty$ $V_{pe}(r)$ becomes the Coulomb potential, $-Z_p/r$. For a finite r_c value $V_{pe}(r)$ is a short-range potential characterized by the interaction length r_c: For large r values it decays exponentially, while for small r values it is Coulombic.

We repeated the CTMC calculations (see Sec. II) with the above model potential by using different values of the interaction length $r_c = 5$, 10 and 100 a.u. The number of the collision events in each case was 2×10^7. The results are plotted in Fig. 3. In part (a) the energy spectra of the forward ejected ($\vartheta_e = 0° \pm 3°$) electrons belonging to different interaction lengths are seen. In part (b) the longitudinal momentum centroids of the recoil target ion obtained for different r_c values are shown as a function of the energy loss of the projectile. Comparing parts (a) and (b) one may conclude that while the cusp peak dramatically decreases with decreasing interaction length (corresponding to smaller strength of PCI), for the $p_{t\|}$ momentum centroid one can observe only small changes.

The above result means that the longitudinal momentum centroid of the recoil target ion contains less information about the electron cusp than the electron energy spectrum (or momentum distribution). In the following we show that the dependence of the $p_{t\|}$ momentum centroid on the projectile energy loss is rather determined—besides the kinematical effects discussed above—by two-center effects. These latter effects cannot be separated by CTMC calculations, they are present even for the smallest interaction length investigated in the present work, $r_c = 5$ a.u. However, information about the two-center effects can be obtained by comparing the results of CDW-EIS calculations with those of a *one-center* theory, the first-Born ($B1$) approximation. Such a comparison is made in Fig. 4. One can establish a large difference between the momentum centroids predicted by the two theories: The $B1$ results do not show any singularity at the energy-loss value corresponding to $v_e = v_p$, and the minimum value of the $p_{t\|}$ momentum centroid is considerably larger in this case than for CDW-EIS.

In $B1$ discussed above the final continuum states are centerd at the target atom. Within the first-Born approximation one can formulate another one-center theory by choosing *projectile-centered* continuum states for the final states. We denote the latter approximation by $B1(P)$. This is known to account for the ECC process, but due to the one-center character of the theory it predicts a symmetric electron cusp. We used also $B1(P)$ to calculate the momentum centroids of the recoil target and the electron. The obtained values (for $p_{t\|}$ see Fig. 4) are very close to the CDW-EIS results for projectile energy-loss values around the matching point $v_e = v_p$, indicating that in this range the projectile-centered continuum states play a more important role than the target-centered ones. At the same time, $B1(P)$ is unable to describe the low-energy electron emission: In Fig. 4 the $B1(P)$ curve shows an increasing deviation from the kinematical limit with decreasing ΔE_p values. This behavior is opposite to the experimental observation (see Fig. 1). We may conclude that in a correct description one has to include both the target- and projectile-centered continuum states.

Furthermore, neither of $B1$ and $B1(P)$ can reproduce the sudden change of the momentum centroids observed in the experiment just above $v_e = v_p$ (see Fig. 1). Again, this feature

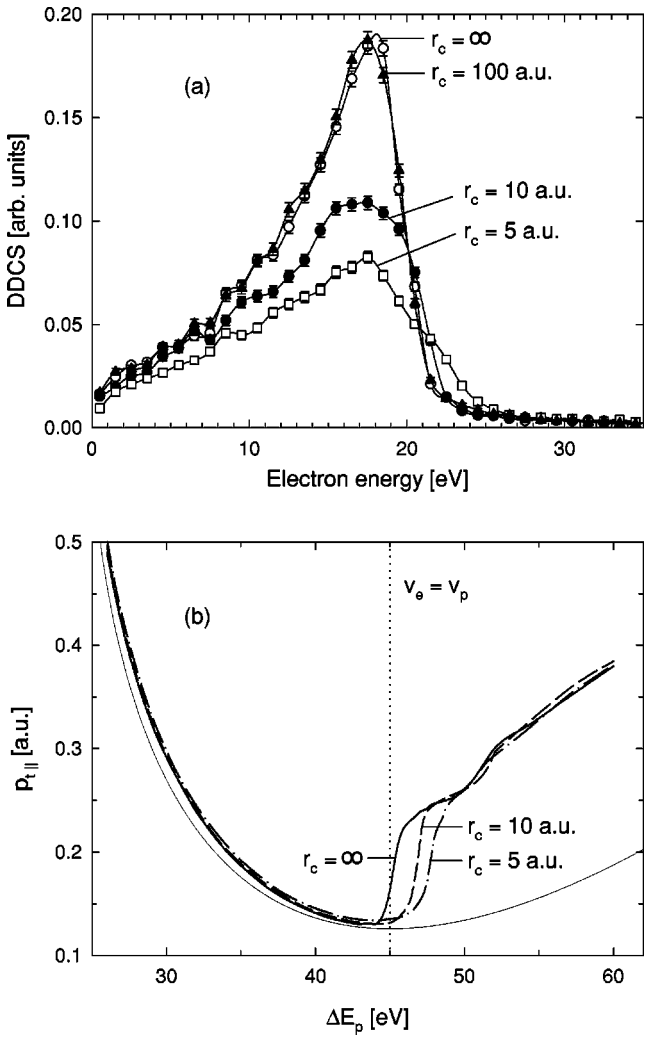

FIG. 3. Results of CTMC calculations performed with a model potential for the projectile-electron interaction defined by Eq. (11). (a) Energy spectra of the electron cusp belonging to interaction length values of $r_c = 5$ arb. units (open squares), $r_c = 10$ arb. units (full circles), $r_c = 100$ arb. units (full triangles), and $r_c = \infty$ (open circles). (b) The centroid of the longitudinal momentum distribution of the recoil target ion at $r_c = 5$ arb. units (dashed-dotted line), $r_c = 10$ arb. units (dashed line), and $r_c = \infty$ (solid line). The thin solid line denotes the kinematical limit.

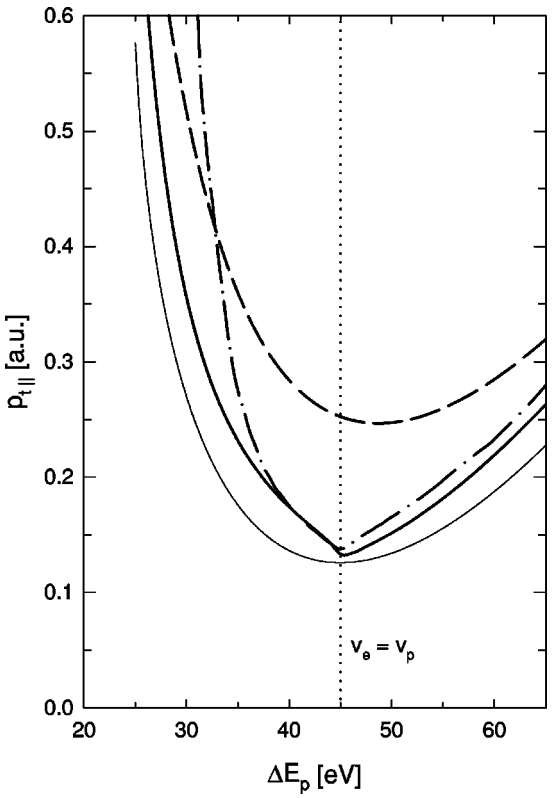

FIG. 4. The centroid of the longitudinal momentum distribution of the recoil target ion. The notations of the curves: solid line, CDW-EIS; dashed line, first-Born approximation with target-centered continuum states; dashed-dotted line, first-Born approximation with projectile-centered continuum states; thin solid line, kinematical limit.

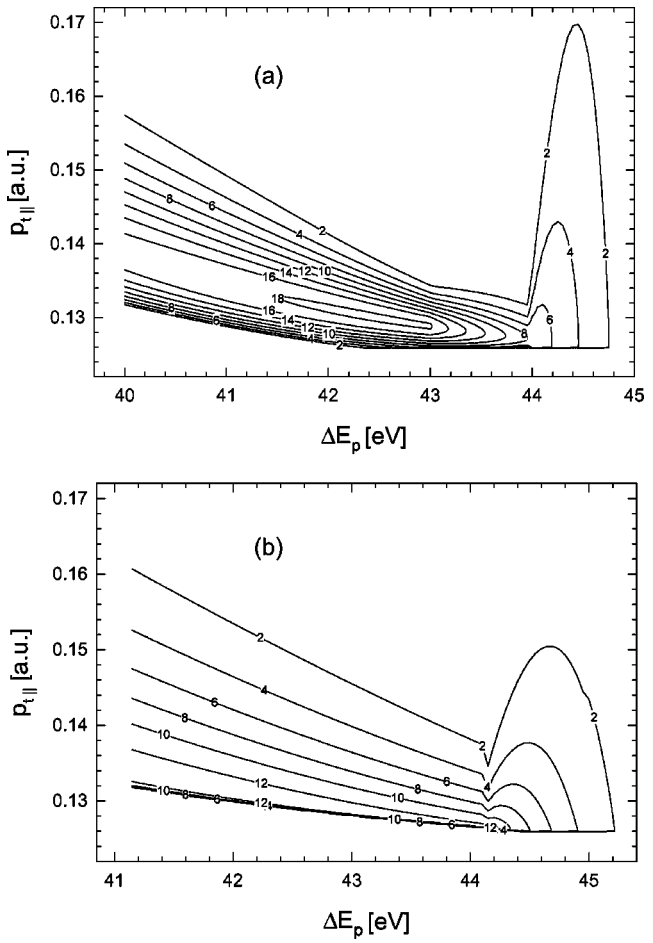

FIG. 5. Contour plots of the longitudinal momentum distribution of the recoil target ion calculated by the CTMC method applying (a) the Coulomb potential and (b) the short-range model potential defined by Eq. (11) with $r_c=5$ arb. units for the projectile-electron interaction. The scale of the plots is linear, the numbers at the contour-lines show relative intensities.

of the momentum centroids can probably be explained only by including the continuum of *both* the projectile and the target, i.e., it is a two-center effect.

Now the question arises: Can one obtain new information about PCI by applying the combined technique of the projectile energy-loss spectrometry and the recoil ion momentum spectroscopy? According to Fig. 3, the direct measurement of the electron cusp seems to be a more sensitive way of the study of PCI than the measurement of the centroid of the recoil target ion momentum distribution. To answer the above question, we analyzed the *full* $p_{t\|}$ momentum distribution instead of regarding only its centroids. For this purpose we fitted a function in the plane defined by ΔE_p and $p_{t\|}$ to the ''surface'' of the corresponding triply differential cross sections obtained from the CTMC calculations. The contour plots of the fitted surfaces for interaction lengths of $r_c=\infty$ and $r_c=5$ a.u. are presented in Figs. 5(a) and 5(b), respectively. The difference between the two momentum distributions is very large. The stronger focusing effect in case of the long-range Coulomb potential results in a much narrower momentum distribution compared to the case of the short-range potential. This is in contrast with the small dependence of the momentum centroid as a function of the interaction length, particularly for $\Delta E_p<45$ eV [see Fig. 3(b)].

As a further analysis of the presence of PCI in the momentum distribution of the collision fragments, we determined the momentum centroids for the recoil target ion and the ejected electron as a function of the scattering angle of the projectile. To this we used the CDW-EIS theory. The calculations were made for projectile scattering angles $\vartheta_p=0$, 0.30, 0.48, and 0.67 mrad. The results are summarized in Fig. 6. Interestingly, a small change of ϑ_p gives rise to a large change of the momentum centroids. For $p_{t\|}$ and $p_{e\|}$ the effect is stronger for $\Delta E_p>45$ eV, thereby the singularity caused by PCI at $v_e=v_p$ becomes more pronounced with increasing ϑ_p. The dependence on the projectile scattering angle is particularly strong for the transverse momentum of the ejected electron in the whole regarded range of ΔE_p. The results of this analysis call the attention to a further possible experimental study of PCI: One could obtain valuable information about PCI by repeating the measurements of An *et al.* [9] for *nonzero* projectile scattering angles.

IV. CONCLUSIONS

We applied the CTMC method and the CDW-EIS theory to interpret the experimental data obtained by An *et al.* [9]

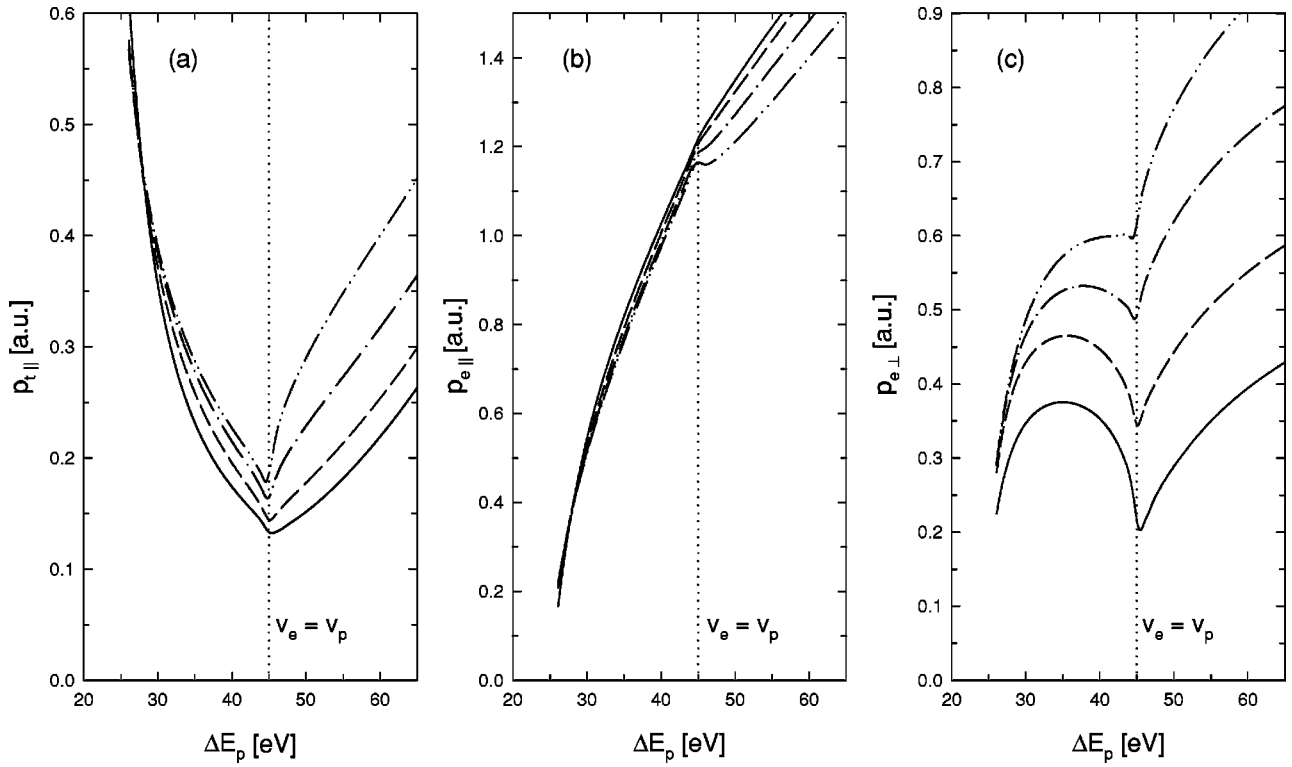

FIG. 6. Results of CDW-EIS calculations for the centroids of the momentum distributions of the recoil target ion and the ejected electron as a function of the projectile energy loss at different values of the projectile scattering angle ϑ_p. (a) and (b) Longitudinal momentum of the target ion and the electron, respectively. (c) Transverse momentum of the electron. The solid, the dashed, the dashed-dotted, and the dashed-dotted-dotted lines belong to values of $\vartheta_p = 0$, 0.30, 0.48, and 0.67 mrad, respectively.

for 75-keV $H_2^+ + He$ collisions. We found a qualitative agreement between the measured and calculated momentum centroid values of the recoil target ion and the ejected electron. We showed that the gross dependence of the longitudinal momentum centroids as a function of the energy loss of the projectile can simply be explained by the kinematical limits of the momentum distributions, and by the fact that the angular distribution of the ejected electron has a maximum close to $\vartheta_e = 0°$ (particularly for electron energies smaller than the cusp energy).

Our calculations confirmed the conclusion of An *et al.* [9] that the rapid changes of the momentum centroids observed in the experiment at the energy-loss value corresponding to the matching velocity $v_e = v_p$ are signatures of PCI. In order to investigate the sensitivity of the momentum centroids to PCI, we repeated the CTMC calculations applying a short-range model potential between the electron and the projectile ion as a function of the interaction length. By varying the interaction length we could change the strength of PCI. We observed only slight changes of the centroid values when the interaction length varied between 5 a.u. and infinity. This finding together with the analysis carried out within the first-Born approximation applying target- and projectile-centered final continuum states indicate that the behavior of the momentum centroids as a function of the energy loss of the projectile is less affected by PCI, rather it is determined—besides the kinematical effects—by the two-center character of the electron emission.

From our CTMC simulations carried out with the short-range potential we also concluded that the measurement of the momentum centroids yields less information about the details of the cusp formation (or, in general, about PCI) than the direct measurement of the electron cusp. At the same time, the high-resolution measurement of the *detailed momentum distributions* would probably be a sensitive way to study PCI effects. Furthermore, on the basis of CDW-EIS calculations we showed that the momentum distributions of the collision fragments depend sensitively on the scattering angle of the projectile, with increasing projectile scattering angle the $v_e = v_p$ singularity becomes more pronounced. Therefore, the extension of the measurements of An *et al.* [9] to nonzero projectile scattering angles would also be a significant step to clarify the role of PCI in ionizing collisions.

ACKNOWLEDGMENTS

This work was supported by the Hungarian Scientific Research Foundation (OTKA, Grant No. T031833) and the National Information Infrastructure Program (NIIF). L. G. gratefully acknowledges the financial support of the Bolyai Research Foundation of the Hungarian Academy of Sciences.

[1] A. Salin, J. Phys. B **2**, 631 (1969).
[2] G.B. Crooks and M.E. Rudd, Phys. Rev. Lett. **25**, 1599 (1970).
[3] J. Macek, Phys. Rev. A **1**, 235 (1970).
[4] P.D. Fainstein, V.H. Ponce, and R.D. Rivarola, J. Phys. B **24**, 3091 (1991).
[5] T. Vajnai, A.D. Gaus, J.A. Brand, W. Htwe, D.H. Madison, R.E. Olson, J.L. Peacher, and M. Schulz, Phys. Rev. Lett. **74**, 3588 (1995).
[6] M. Schulz, T. Vajnai, A.D. Gaus, W. Htwe, D.H. Madison, and R.E. Olson, Phys. Rev. A **54**, 2951 (1996).
[7] R. Moshammer, J. Ullrich, H. Kollmus, W. Schmitt, M. Unverzagt, H. Schmidt-Böcking, C.J. Wood, and R.E. Olson, Phys. Rev. A **56**, 1351 (1997).
[8] T. Weber, Kh. Khayyat, R. Dörner, V.D. Rodriguez, V. Mergel, O. Jagutzki, L. Schmidt, K.A. Müller, F. Afeneh, A. Gonzalez, and H. Schmidt-Böcking, Phys. Rev. Lett. **86**, 224 (2001).
[9] L. An, Kh. Khayyat, and M. Schulz, Phys. Rev. A **63**, 030703 (2001).
[10] J. Ullrich, R. Moshammer, R. Dörner, O. Jagutzki, V. Mergel, H. Schmidt-Böcking, and L. Spileberger, J. Phys. B **30**, 2917 (1997).
[11] A.E.S. Green, D.L. Sellin, and A.S. Zachor, Phys. Rev. **184**, 1 (1969).
[12] R.H. Garvey, C.H. Jackman, and A.E.S. Green, Phys. Rev. A **12**, 1144 (1975).
[13] K. Tőkési and T. Mukoyama, Bull. Inst. Chem. Res., Kyoto Univ. **72**, 62 (1994).
[14] K. Tőkési, L. Sarkadi, and T. Mukoyama, J. Phys. B **30**, L123 (1997).
[15] K. Tőkési and G. Hock, Nucl. Instrum. Methods Phys. Res. B **124**, 398 (1997).
[16] K. Tőkési and Á. Kövér, J. Phys. B **33**, 3067 (2000).
[17] L. Sarkadi, U. Brinkmann, A. Báder, R. Hippler, K. Tőkési, and L. Gulyás, Phys. Rev. A **58**, 296 (1998).
[18] L. Sarkadi, K. Tőkési, and R.O. Barrachina, J. Phys. B **33**, 847 (2000).
[19] L. Sarkadi, L. Lugosi, K. Tőkési, L. Gulyás, and Á. Kövér, J. Phys. B **34**, 4901 (2001).
[20] R. Abrines and I.C. Percival, Proc. Phys. Soc. London **88**, 861 (1966).
[21] R.E. Olson and A. Salop, Phys. Rev. A **16**, 531 (1977).
[22] P.D. Fainstein, L. Gulyás, and A. Salin, J. Phys. B **29**, 1225 (1996).
[23] P.A. Závodszky, L. Gulyás, L. Sarkadi, T. Vajnai, Gy. Szabó, S. Ricz, J. Pálinkás, and D. Berényi, Nucl. Instrum. Methods Phys. Res. B **86**, 175 (1994).
[24] C.O. Reinhold and R.E. Olson, Phys. Rev. A **39**, 3861 (1989).